Saudi Journal of Biological Sciences 26 (2019) 1364–1371

Contents lists available at ScienceDirect

Saudi Journal of Biological Sciences

journal homepage: www.sciencedirect.com

Original article

Green synthesis of ZnO hierarchical microstructures by *Cordia myxa* and their antibacterial activity

Sadia Saif [a,b,c,*], Arifa Tahir [b], Tayyaba Asim [b], Yongsheng Chen [a], Mujeeb Khan [d], Syed Farooq Adil [d,*]

[a] School of Civil and Environmental Engineering, Georgia Institute of Technology, Atlanta, GA 30332, USA
[b] Department of Environmental Science, Lahore College for Women University, Lahore 54000, Pakistan
[c] Department of Environmental Sciences, Kinnaird College for Women, Lahore 54000, Pakistan
[d] Department of Chemistry, College of Science, King Saud University, P.O. Box 2455, Riyadh 11451, Saudi Arabia

ARTICLE INFO

Article history:
Received 9 July 2018
Revised 2 January 2019
Accepted 6 January 2019
Available online 7 January 2019

Keywords:
ZnO microstructures
Solution combustion
Leaves mediated
Antibacterial activity

ABSTRACT

In this study, the leaves extract of *Cordia myxa*, has been used for the first time to synthesize zinc oxide (ZnO) hierarchical microstructures. The solution combustion method was employed as a self-sustaining reaction between zinc nitrate and the leaves extract. The surface properties of leaves mediated ZnO microstructures were determined by UV–Visible spectral analysis, Fourier transform infrared (FT-IR), Cold field emission-scanning electron microscopy (CFE-SEM), Energy dispersive X-ray (EDX), X-ray diffraction (XRD) and X-ray photoelectron spectroscopy (XPS). In addition, the effect of the leaves extract concentration on ZnO structures, size and surface properties was also studied. ZnO structures synthesized employing *C. myxa* were found to be hexagonal, triangular and round in shape which was determined using CFE-SEM. X-ray diffraction (XRD) analysis confirmed the crystalline nature of compounds. Furthermore, *C. myxa* mediated ZnO microstructures shows good bactericidal activity against Gram-negative (*Escherichia coli*) and Gram-positive (*Staphylococcus aureus*) bacteria.

1. Introduction

Among metal oxides, zinc oxide (ZnO) nano/micro-structures have attracted considerable interest in the field of engineering as well as in optical, chemical, mechanical, and biological sciences due to their unique functions and stimulation characteristics (Zhang et al., 2009; Zhao et al., 2014). Fascinating properties of ZnO due to their high surface area make it a remarkable agent for various applications like electronics (biosensing and biodetection) (Dagdeviren et al., 2013), gas sensors fuel production (Wang et al., 2012), cosmetics (Cross et al., 2007) and environmental protection (Zhou et al., 2006). It's environmental friendly property and biocompatibility makes it desirable especially for biomedical applications and therapeutic intervention, such as drug delivery and nanomedicine (Rasmussen et al., 2010), biological sensing/bioimaging (Xiong, 2013), biological labeling, gene delivery, DNA delivery cell culturing (Nie et al., 2006), anti-diabetic activities (Alkaladi et al., 2014), antibacterial defense (Applerot et al., 2009), antifungal protection (Sharma et al., 2010) and pediculocidal/larvicidal control (Kirthi et al., 2011).

Several approaches such as chemical precipitation (Dakhlaoui et al., 2009; Raoufi, 2013), sol–gel spin coating (Vafaee and Ghamsari, 2007), spray pyrolysis (Lee et al., 2012), thermal decomposition (Baskoutas et al., 2007; Yi et al., 2008) and electrochemical techniques (Pourmortazavi et al., 2015) have been developed to synthesize the nano/micro-structure of ZnO (Li and Wang, 2009; Qiu et al., 2010; Song et al., 2012). Recently, owing to the biological importance of the ZnO nano/micro-structure, synthesis of these materials using eco-friendly routes has gained considerable attention. So far, great deal of effort has been devoted towards exploring the green synthesis routes which is an efficient alternative to chemical and physical methods. The green synthesis of bioactive ZnO nano/micro-structures from various plant resources and their antibacterial, antifungal and photocatalytic activities have been documented by many researchers (Lakshmeesha et al., 2014;

* Corresponding authors at: Department of Environmental Sciences, Kinnaird College for Women, Lahore 54000, Pakistan (S. Saif); Department of Chemistry, College of Science, King Saud University, P.O. Box 2455, Riyadh 11451, Saudi Arabia (S.F. Adil).
E-mail addresses: sadia.saif@kinnaird.edu.pk (S. Saif), sfadil@ksu.edu.sa (S.F. Adil).

Peer review under responsibility of King Saud University.

Production and hosting by Elsevier

https://doi.org/10.1016/j.sjbs.2019.01.004
1319-562X/

Tripathi et al., 2014; Yuvakkumar et al., 2014; Kavyashree et al., 2015; Odoom-Wubah et al., 2016; Udayabhanu et al., 2016).

Among various green synthesis methods, solution combustion synthesis (SCS) is a facile, cost effective and environmental friendly approach for the synthesis of nanocrystalline metal oxides using an appropriate precursor (metal salt) and fuel (reducing agent). Generally, metal nitrates are preferred over other salts as the oxidizing agent due to their solubility, thus resulting in a highly homogeneous solution. Many studies have been revealed that carbohydrates, amines, sugar, urea and glycine can be used as a fuel to prepare nanocrystalline ZnO (Dinesha et al., 2009; Amdad et al., 2013).

Recently, the trend of preparing metal/metal oxides NPs using the extracts of various plants has gained popularity. So far, several plants such as, *Pulicaria glutinosa*, *Salvadora persica L.* and so on have been employed for this purpose (Al-Marri et al., 2015; Fazlzadeh et al., 2017). Apart from these, different plants from the genus *Cordia* such as Cordia *dichotoma and Cordia myxa,* which are widely distributed in regions of tropical and subtropical climates such as Central and South America, Asia and Africa (Schmelzer and Gurib-Fakim, 2008), have also been applied for the synthesis of nanoparticles (Kumari et al., 2016). However, to the best of our knowledge, *Cordia myxa* L. which is another plant of the genus *Cordia*, has not been used so far for the preparation of nanoparticles. This plant, belongs to the family Boraginaceae and exhibit excellent biological, and pharmacological properties (Ghazanfar, 1994; Ficarra et al., 1995). The phytochemical studies have reveal the presence of flavonoids, alkaloids, saponins, sterols and terpenes in leaves and fruits of *Cordia myxa L.* plant. Particularly, the *Cordia* leaves extract has shown significant antioxidant activity due to the presence of many phenolic derivatives such as chlorogenic and caffeic acid (Aberoumand and Deokule, 2009; Matias et al., 2015).

In this study, a SCS approach was adopted for the synthesis of ZnO utilizing *Cordia myxa L.* leaves extract as fuel (reducing agent) with an aim to prepare a uniform, ultrafine ZnO using a process that saves time and energy. It is assumed that phenolic contents in *C. myxa* extract may act as a reducing agent during solution combustion synthesis for the production of ZnO. This study places special emphasis on detailed characterization of *C. myxa* mediated ZnO structures. The effect of extract concentration on ZnO morphology and sizes was evaluated. Furthermore, potential toxicity of resultant ZnO nanomaterials were investigated against selected microbial pathogens.

2. Materials and methods

2.1. Materials and chemicals

Cordia myxa leaves were collected from Bagh-e-Jinnah, Lahore Pakistan. Zinc nitrate hexahydrate (Zn $(NO_3)_2{\cdot}6H_2O$), Muller Hinton Agar and 69% HNO_3 were purchased from Sigma Aldrich. Milli-Q water (Millipore Sigma Aldrich) was used throughout the reaction process.

2.2. Preparation of extract

The *C. myxa* leaves extract (LE) was prepared by the following procedure. *C. myxa* leaves were cleaned with tap water followed by distilled water and dried in the shade. The dried material was ground and passed through a 20 mesh sieve. Extract was prepared by the maceration method. 20 g of dry leaves powder was macerated in 200 mL of water at 30–33 °C with occasional shaking (Vongsak et al., 2013). The extract was filtered, and then the same process was repeated until the extraction was exhausted. Double filtration was done by using Whatmann filter paper for removal of any solid residue. Finally, a stock solution containing 0.1 mg/ml of *C. myxa* leaves extract was obtained.

2.3. Synthesis of zinc oxide (ZnO)

ZnO microstructures were prepared by solution combustion synthesis (SCS) using zinc nitrate and *C. myxa* leaves extract as a fuel (Lakshmeesha et al., 2014). In this study, three different concentrations of extract were used (i) pure extract (0.1 mg/ml), 25% extract (prepared by mixing 25 mL pure extract and 75 mL water), and 10% extract (prepared by 10 mL pure extract + 90 mL water). In order to prepare the zinc based microstructures from pure extract, 4.5 g of $Zn(NO_3)_2{\cdot}6H_2O$ (15 mmol) was taken in 20 mL of stock solution of leaves extract, the mixture was thoroughly stirred using a magnetic stirrer to make a homogenous mixture at 60 °C. This mixture was subjected to calcination in a preheated furnace at 400 °C for 2 h. The obtained milky white ZnO product was stored in a dry container in a dry place for further analysis (Fig. 1). Similarly, the reactions with diluted extract were also performed using 20 mL of aqueous leaves extract from the aforementioned diluted stock solutions. The product obtained was labeled as **ZnO-P** (obtained using pure extract), **ZnO-10** (prepared by using 10% extract), **ZnO-25** (prepared by using 25% extract).

2.4. Characterization measurements

Absorption spectra of samples were measured by the UV–Visible spectrophotometer (UV-1800; Shimadzu, Tokyo, Japan).). Morphology, size and microstructures of resultant ZnO product were studied using cold field emission scanning electron microscopy (CFE-SEM, SU8230, Hitachi, Tokyo, Japan) equipped with EDX. Samples were dried at 60 °C for at least 24 h before testing. Chemical binding of synthesized zinc oxide products were analyzed using a Fourier transform infrared (FTIR) spectrometer (Perkin Elmer, Spectrum 400, Walthman, MA, USA) equipped with an attenuated total reflection (ATR) attachment. Samples were placed on the sample holder, and all spectra were recorded in a wave number ranging from 4000 to 650 cm^{-1} by cumulating 20 scans at a resolution of 4 cm^{-1}. Crystalline nature of plant mediated ZnO was identified by X-ray powder diffraction patterns (Bruker D8 Advance, Germany) using Cu K_α radiation (λ = 1.54 Å) source. The Thermo Scientific™ K-Alpha+™+ X-ray Photoelectron Spectrometer (XPS) System (Thermo Fisher Scientific, Waltham, MA, USA) was used to study the near-surface elemental composition of ZnO samples. Survey spectra were collected over 0–1350 eV, with a high-resolution scan of 0.1 eV.

2.5. Antibacterial assay

The antibacterial activity of synthesized ZnO microstructures was evaluated against Gram-positive (*Staphylococcus aureus*) and Gram-negative (*Escherichia coli*) strains using the disk-diffusion method. Agar plates were prepared with 15–20 mL of sterile Muller Hinton Agar for bacteria and allowed to stand for 2 h. 10.0 μL of 24 h broth culture of bacterial species were swabbed on the top of the solidified agar plates and allowed to dry. Three different concentrations (50 μg/mL, 100 μg/mL, and 200 μg/mL) of synthesized ZnO product were used for antibacterial assay. Whatman paper discs were soaked in colloidal solutions of ZnO for 30 min. The loaded disks were placed on the surface of the agar plates. Water was used as a solvent. Negative control was without ZnO. All the plates were then incubated at 37 °C for bacteria for 24 hr. The sensitivity was recorded by measuring the clear zone of growth inhibition on agar surface around the disks in millimeter. Experiments were performed in triplicates.

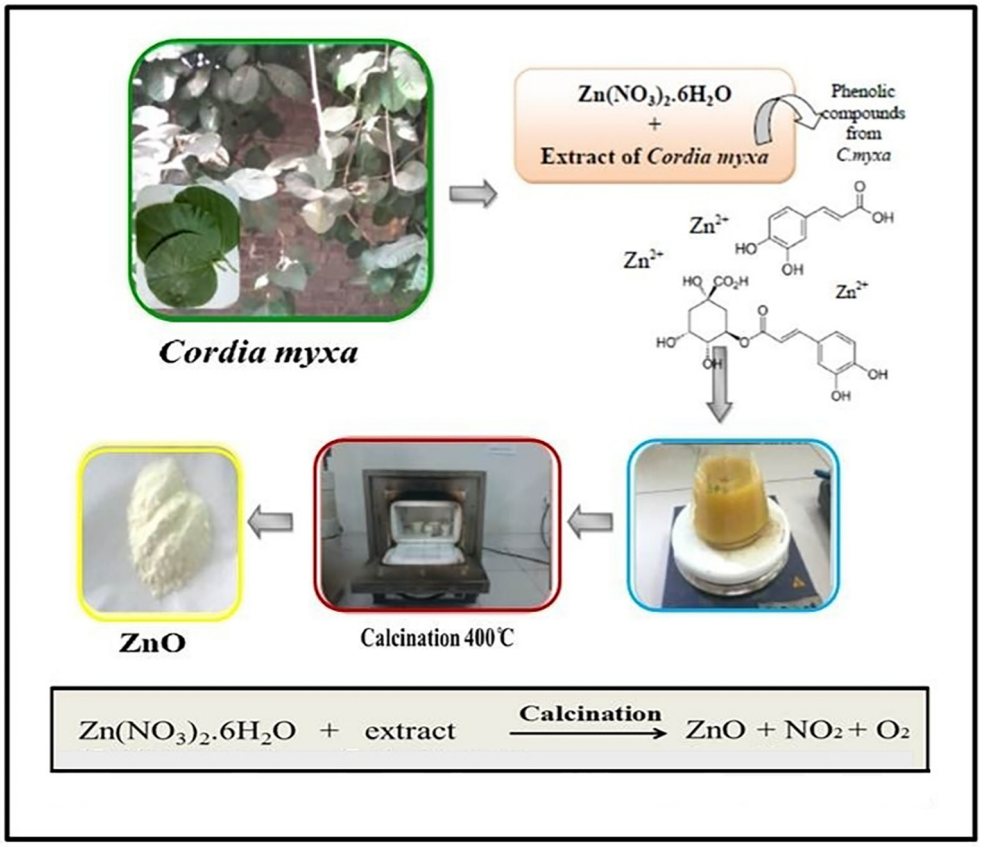

Fig. 1. Schematic representation of the synthesis of ZnO microstructures and reaction mechanism.

3. Results and discussion

This study reports the green synthesis of crystalline ZnO microstructures using aqueous leaves extract of *C. myxa* by employing solution combustion method. The effect of extract concentration on characteristics of synthesized ZnO and their bactericidal activity has been investigated as well.

3.1. UV–Vis spectroscopy

Fig. 2 shows the absorption spectra of pure leaves extract and as-prepared ZnO using different concentrations of *C. myxa* leaves extract. The narrow peak obtained at 273 nm is attributed to the UV absorption of polyphenols present in leaves extract. All the samples exhibited strong UV absorption spectra with the absorption peak ranging from 340 to 370 nm, which appears due to the surface plasmon resonance of ZnO which indicates the formation of the desired ZnO as reported previously (Sangeetha et al., 2011; Lakshmeesha et al., 2014; Ramesh et al., 2015). It was observed that the concentration of leaves extract has significant effect on the formation of ZnO microstructures. Notably, a broad absorption peak at 368 nm is obtained when the pure extract is employed. However, upon dilution of leaves extract with water, the absorption peak is shifted to the lower wavelength from 368 nm to 354 and 342 nm in case of ZnO obtained from 25% and 10% leave extract, respectively. Apart from the red-shift, the peak intensity also increased by increasing the extract concentration as seen in Fig. 2. The band gap energy corresponds to the absorption limit, which was roughly estimated by the following equation:

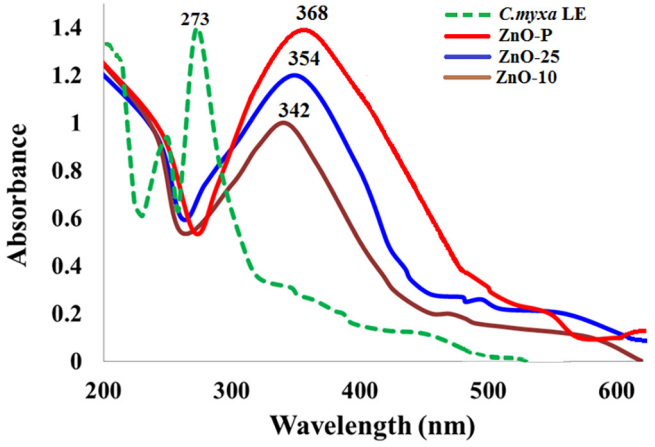

Fig. 2. UV–Vis absorption spectra of ZnO synthesized employing different concentrations of *C. myxa* leaves extract.

$$Eg = \frac{hc}{\lambda} eV \quad (1)$$

$$Eg = \frac{1240}{\lambda} eV \quad (2)$$

where Eg is the band gap energy (eV), h is Planck's constant (6.62×10^{-34}Js), c is the light velocity (3×10^{8} m/s) and λ is the wavelength (nm). The band gap energy for the ZnO samples obtained by using different concentration of leaves extract were calculated 3.36 eV, 3.5 eV, and 3.62 eV, in case of pure, 25% and 10% leaves extract.

3.2. FT-IR spectroscopy

Biomolecules of *C. myxa* responsible for the reduction of zinc salt to metallic zinc oxide was identified through particular vibration peaks at different wave numbers by FTIR spectroscopy. Fig. 3 (a) spectra represents the possible biomolecules present in aqueous leaves extract of *C. myxa*. A broad peak at 3328 cm^{-1} representing the hydroxyl groups, confirms the presence of phenols; while a sharp peak at 2920 cm^{-1} corresponds to the stretching of C—H bonds of aliphatic groups. The absorption peak around 1656 cm^{-1} is due to aromatic bending of the alkene (C=C) group, whereas a 1,244 cm^{-1} strong bands is related to the stretching of C—O group in ether. Furthermore, the sharp absorption peak at 1047 cm^{-1} and a weak band at 807 cm^{-1} represents the stretching of primary alcohol (OH) and bending of C—H of aromatics group. All these IR peaks clearly points towards the presence of flavonoids and polyphenolic phytomolecules.

The interactions between the phytomolecules of *C. myxa* leaves extract and surface of ZnO is demonstrated by the FT-IR spectra as shown in Fig. 3. FTIR spectra exhibit several intense peaks corresponding to various functional groups of the phytomolecules of the leaves extract. Such as, a strong band at 3280 cm^{-1}, due to stretching vibrations of O—H groups of phenols. All these peaks are almost similar to the peaks demonstrated in the IR spectrum of pure leaves extract, except some marginal shift in their peak position and variation in the intensity. This strongly suggests the little coating of the phytomolecules of the leaves extract on the surface of the resultant ZnO particles. Notably, the sample prepared by high concentration of leaves extract i.e. pure extract demonstrated the presence of phytomolecules as compared to the other samples prepared at lower concentrations (Fig. 3d). This is further confirmed by XPS analysis the details of which are given below.

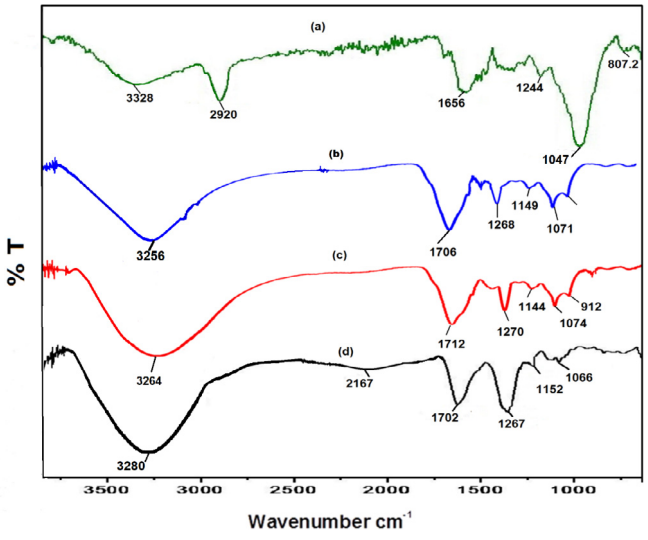

Fig. 3. FTIR spectra of (a) *C. myxa* leaves extract (b) ZnO-10 (c) ZnO-25 (d) ZnO-P.

3.3. CFE-SEM and EDX analysis

Morphology of *C. myxa* synthesized ZnO samples were also characterized by cold field emission scanning electron microscope (CFE-SEM). Images of ZnO are shown in Fig. 4 (a, b, c). Hexagonal wurtzite structures were obtained when pure extract was used; the images clearly indicate that the structure consists of clusters of symmetrically arranged small hexagonal plates. At 25% extract concentration, wurtzite shaped particles were obtained, which comprised of micro or nano size triangular entities. Whereas at lower extract concentration (10%), spherical shaped particles comprising of layer-by-layer discs like entities were observed as shown in Fig. 4c. Further analysis by energy dispersive X-ray (EDX) spectrometer confirmed the presence of ZnO (Fig. 5). The weight percentage of zinc and oxygen was found to be analogous for all samples of ZnO.

3.4. X-ray diffraction study

Fig. 6 shows the XRD patterns of ZnO microstructures synthesized by *C. myxa* leaves extract with different concentrations. The sharp diffraction peaks reveal the crystalline nature of the as-prepared materials. The prominent peaks at 31.66°, 34.42°, 36.02°, 47.53°, 56.56°, 62.86°, 67.85°, 69.42, 72.14° and 76.40° correspond to the (1 0 0), (0 0 2), (1 0 1), (1 0 2), (1 1 0), (1 0 3), (2 0 0), (1 1 2), (2 0 1) and (0 0 4) planes, confirming the formation of wurtzite structure and well matched with JCPDS (Card No: 36-1451) (Suresh et al., 2015b).

3.5. High resolution X-ray photoelectron spectroscopy (XPS)

The high resolution XPS spectra of the as-prepared ZnO are shown in Fig. 7. The survey of XPS spectrum clearly revealed that the product was ZnO. High binding energy of element zinc, Zn_2p_3, was observed by two sharp peaks around 1021.38 ± 0.3 eV and 1044.58 ± 0.2 eV for all samples. Binding energies around 531.06 ± 1.0 eV of the prepared samples could be attributed to lattice oxygen of ZnO. However, the low intensity signals of carbon (C) element were observed in ZnO sample synthesized with pure extract. This may be due to the presence of carbon in the form of

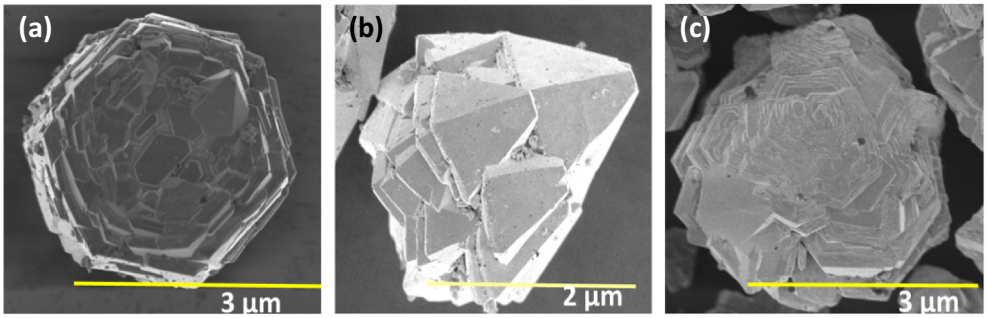

Fig. 4. SEM images of synthesized ZnO microstructures (a) ZnO-P (b) ZnO-25 (c) ZnO-10.

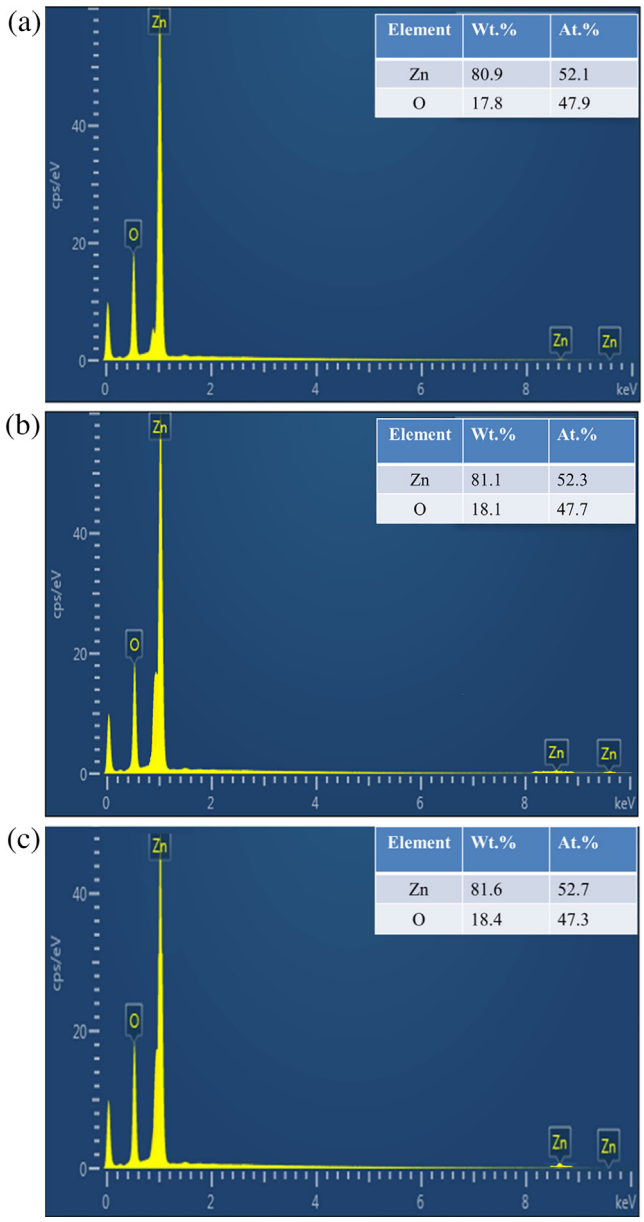

Fig. 5. . EDX profile of *C. myxa* synthesized (a) ZnO-P (b) ZnO-25 (c) ZnO-10.

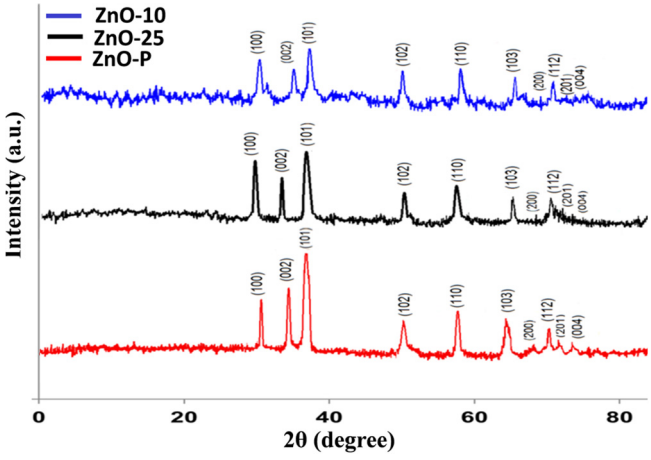

Fig. 6. XRD pattern of synthesized ZnO microstructures.

phytomolecules on the surface of ZnO particles prepared from pure extract, which was also confirmed from the FT-IR spectroscopy.

3.6. Antibacterial bioassay

In this study, bactericidal activity of *C. myxa* synthesized crystalline ZnO microstructures was investigated against both gram-positive (*Staphylococcus aureus*) and gram-negative (*Escherichia coli*) using disc diffusion method. The antibacterial activity of prepared ZnO samples were tested towards bacteria in a dose-dependent manner and values of zone inhibition obtained from assay are presented in Tables 1a and 1b. All synthesized ZnO samples showed substantial growth inhibition against Gram-positive and Gram-negative bacteria.

ZnO hexagonal wurtzite structures synthesized from pure extract i.e. ZnO-P showed prominent activities against *S. aureus* (19.64 ± 0.52 mm) and *E.coli* (17.66 ± 0.46 mm) at the concentration of 200 μg/mL. Moreover, the maximum zone of inhibition was recorded for *E. coli* which was 8.0 ± 0.54 mm, 12.68 ± 0.50 mm and 19.00 ± 0.60 mm at concentrations of 50 μg/mL, 100 μg/mL and 200 μg/mL respectively by ZnO-25. Likewise, ZnO-25 had the highest antimicrobial activity against *S. aureus,* the zone of inhibition ranged from 9.4 ± 0.20 to 23.63 ± 0.68 mm at different concentrations of ZnO. Antibacterial activity of prepared ZnO against *S. aureus* and *E. coli* by changing the ZnO dosage can be seen clearly in Fig. 8. A zone of inhibition of 14.00 ± 0.86 mm and 16.60 ± 0.40 mm was recorded for *E. coli* and *S. aureus*, respectively for ZnO-10 at dosage of 200 μg/mL. It can be observed that *S. aureus* is more susceptible to ZnO as compared to *E.coli* and the results are in confirmation with the several previous researches (Senthilkumar and Sivakumar, 2014; Bhuyan et al., 2015; Qian et al., 2015; Suresh et al., 2015a). The discrepancy in antibacterial activity among the Gram-positive and Gram-negative could be due to difference in bacterial cell wall compositions and the membrane structure (Yuvakkumar et al., 2014).

It is found that the higher concentration of ZnO leads to growth inhibition in both Gram-positive and Gram-negative bacteria as reported by Dutta et al. (2013) who employed higher concentration of ZnO i.e. 175 mg/L against *E. coli* bacterial strains, it was believed that with high amount of reactive oxygen species (ROS) was produced when increasing concentrations of ZnO, which leads to the phenomena of lipid peroxidation (Zhang et al., 2007). It is thought that increasing concentration may damage the bacterial cell membrane, resulting in a leakage of intracellular contents and eventually directing to the death of bacterial cells. Furthermore, the free zinc ion from ZnO has also been found to be responsible for the toxicity in bacterial cells (Li et al., 2011).

Bactericidal property of ZnO toward bacterial species depends on various factors such as particle size, ion dissolution, concentration, morphology, specific surface area, etc. (Li et al., 2011; Raghupathi et al., 2011; Azam et al., 2012; Sharma et al., 2016). Several researchers have found that the toxicity relates to particle size, smaller the particle size higher would be the antibacterial activity (Raghupathi et al., 2011; Azam et al., 2012; Rajiv et al., 2013), however, the results of the present study differ from the previous reports. In one study, Elumalai et al. (2015) synthesized ZnO spherical nanoparticles with an average size of 12 nm utilizing extract of *Murraya koenigii* and tested antibacterial activity against *S. aureus* and *E. coli.* Though, the antibacterial activity of nanosize particles was found to be less as compared to *C. myxa* synthesized ZnO micro particles as described in this study at similar dosage regimes of ZnO. Results of present study clearly display that the morphology and structures of crystalline ZnO influence on antibacterial activity, however it is independent of its size.

The relation of bacterial toxicity with the morphology of crystallite ZnO has been described in few recent researches (Talebian

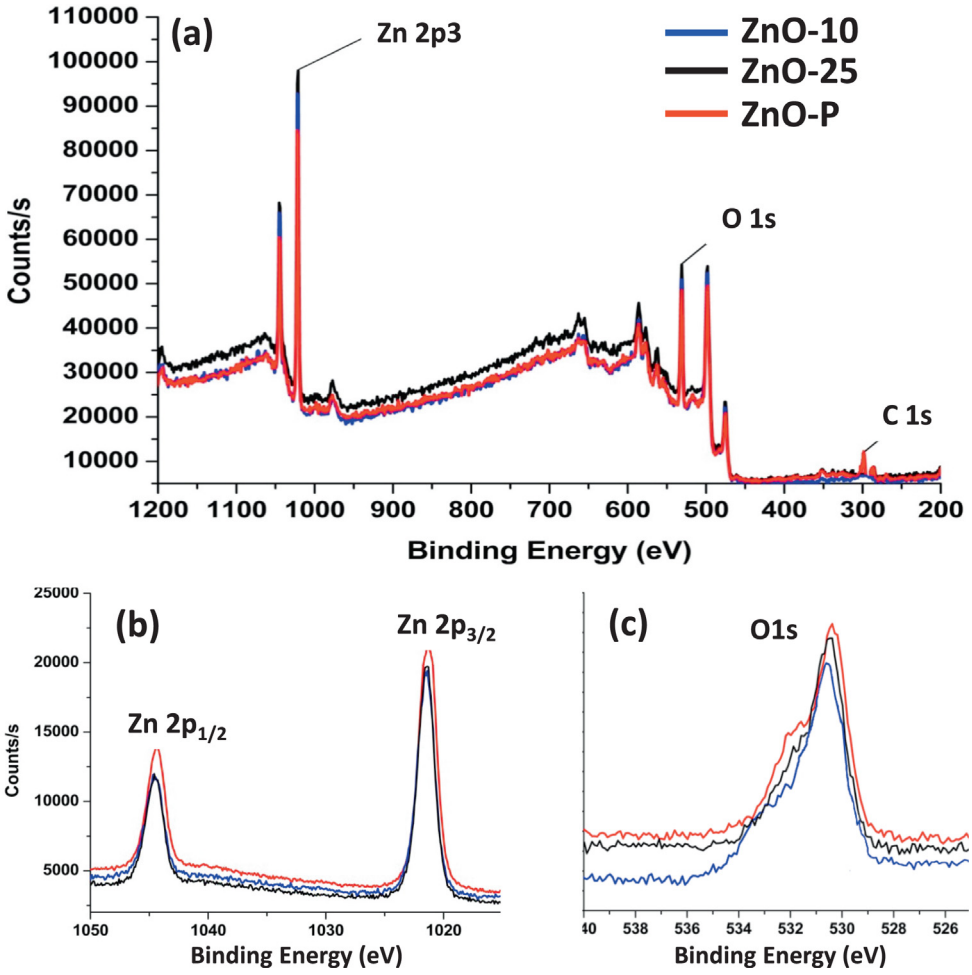

Fig. 7. (a) XPS survey spectra of ZnO microstructures mediated by different concentrations of *C. myxa* extract (b) Zn 2p scan; (c) O 1s scan.

Table 1a
Antibacterial activity of ZnO nano/microstructures against *E.coli* at different dosage regimens.

ZnO microstructures	Morphology	Zone of inhibition(mm) Concentration of ZnO (μg/mL)		
		50	100	200
ZnO-P	Hexagonal	7.2 ± 0.68	11.4 ± 0.74	17.66 ± 0.46
ZnO-25	Pyramid	8.0 ± 0.54	12.68 ± 0.50	19.00 ± 0.60
ZnO-10	Round	6.0 ± 0.80	9.2 ± 1.02	14.00 ± 0.86

Mean ± standard deviation.

Table 1b
Antibacterial activity of ZnO nano/microstructures *S. aureus* at different dosage regimens.

ZnO microstructures	Morphology	Zone of inhibition(mm) Concentration of ZnO (μg/mL)		
		50	100	200
ZnO-P	Hexagonal	8.00 ± 1.00	2.00 ± 0.22	19.64 ± 0.52
ZnO-25	Pyramid	9.4 ± 0.20	15.08 ± 0.30	23.63 ± 0.68
ZnO-10	Round	7.2 ± 0.80	10.8 ± 0.45	16.60 ± 0.40

Mean ± standard deviation.

et al., 2013; Lakshmeesha et al., 2014; Sirelkhatim et al., 2015), which suggest that the generation of reactive oxygen species (ROS) by ZnO is associated with the structural, morphological and optical properties. In the present study, it was observed that the spherical structure of ZnO-10, displayed scanty antibacterial activity against both in Gram-positive and Gram-negative bacterial as compared to other ZnO microstructures of varying morphologies.

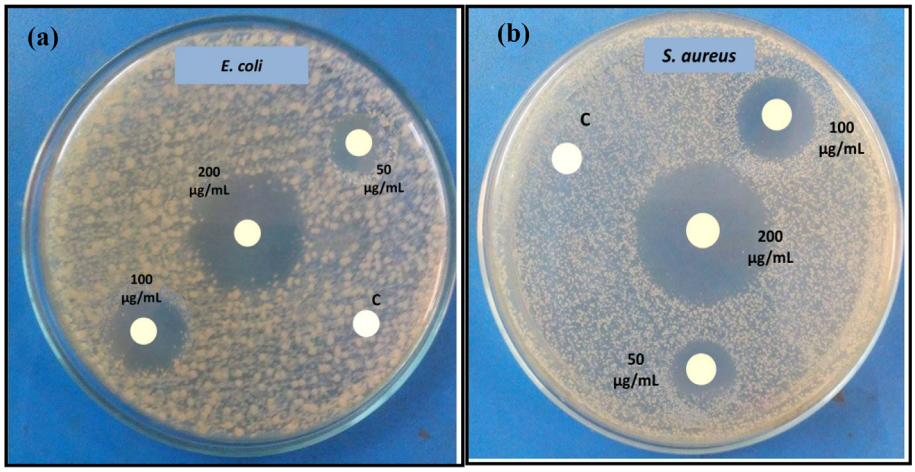

Fig. 8. Antibacterial activity of ZnO-P nano/microstructures against. (a) *E.coli* and (b) *S. aureus.*

4. Conclusions

This study reports the synthesis of ZnO microstructures by aqueous leaves extract of *C. myxa*. The solution combustion method was adopted as a low cost, environmental friendly process in which the oxidizer was nitrate salt and the leaves extract was used as fuel. Different concentrations of extract were employed to synthesize unique ZnO structures. Furthermore, a detailed characterization was part of the physical and chemical analysis of obtained ZnO product. The appearance of broad optical absorption peak of UV–Visible spectral analysis confirmed the synthesis of ZnO, and the stabilizing role of the biomolecules involved in the formation of ZnO was ascertained by FTIR. The FE-SEM studies confirmed that the concentration of the leaves extract is highly efficient in controlling the shape and size of ZnO structures. Data profile of EDX and XPS confirmed that the synthesized product was pure ZnO, while the XRD pattern showed the crystalline nature of synthesized ZnO. This study showed that the *C. myxa* mediated ZnO microstructures obtained have the potential to display the bactericidal properties against various gram positive and gram negative bacterial strains. Further studies are warranted to understand the role of surface morphology and antibacterial property of the obtained ZnO microstructures which will be carried out in the future.

Acknowledgments

This research was partially supported by the U.S. National Science Foundation (NSF Grant no. CBET-1235166). The authors acknowledge the Daniel Lab School of Civil and Environmental Engineering, Nanotechnology Institute Marcus Nanotechnology at the Georgia Institute of Technology, GA. USA, and the Environmental Science Laboratory of Lahore College for Women University in Lahore, Pakistan.

Conflicts of Interest

The authors declare no conflict of interest.

References

Aberoumand, A., Deokule, S., 2009. Studies on nutritional values of some wild edible plants from Iran and India. Pak. J. Nutrition 8 (1), 26–31.
Al-Marri, A.H., Khan, M., Khan, M., Adil, S.F., Al-Warthan, A., Alkhathlan, H.Z., Tremel, W., Labis, J.P., Siddiqui, M.R.H., Tahir, M.N., 2015. Pulicaria glutinosa extract: a toolbox to synthesize highly reduced graphene oxide-silver nanocomposites. Int. J. Mol. Sci. 16 (1), 1131–1142.
Alkaladi, A., Abdelazim, A.M., Afifi, M., 2014. Antidiabetic activity of zinc oxide and silver nanoparticles on streptozotocin-induced diabetic rats. Int. J. Mol. Sci. 15 (2), 2015–2023.
Amdad, A.M., Rahman, I.M., Quayum, M.E., 2013. Fabrication of ZnO nanoparticles by solution combustion method for the photocatalytic degradation of organic dye. J. Nanostructure Chem 3 (1), 36.
Applerot, G., Lipovsky, A., Dror, R., Perkas, N., Nitzan, Y., Lubart, R., Gedanken, A., 2009. Enhanced antibacterial activity of nanocrystalline ZnO due to increased ROS-mediated cell injury. Adv. Funct. Mater. 19 (6), 842–852.
Azam, A., Ahmed, A.S., Oves, M., Khan, M.S., Habib, S.S., Memic, A., 2012. Antimicrobial activity of metal oxide nanoparticles against Gram-positive and Gram-negative bacteria: a comparative study. Int. J. Nanomed. 7, 6003–6009.
Baskoutas, S., Giabouranis, P., Yannopoulos, S.N., Dracopoulos, V., Toth, L., Chrissanthopoulos, A., Bouropoulos, N., 2007. Preparation of ZnO nanoparticles by thermal decomposition of zinc alginate. Thin Solid Film. 515 (24), 8461–8464.
Bhuyan, T., Mishra, K., Khanuja, M., Prasad, R., Varma, A., 2015. Biosynthesis of zinc oxide nanoparticles from *Azadirachta indica* for antibacterial and photocatalytic applications. Mat. Sci. Semicon Proc. 32, 55–61.
Cross, S.E., Innes, B., Roberts, M.S., Tsuzuki, T., Robertson, T.A., McCormick, P., 2007. Human skin penetration of sunscreen nanoparticles: in-vitro assessment of a novel micronized zinc oxide formulation. Skin Pharmacol. Physiol. 20 (3), 148–154.
Dagdeviren, C., Hwang, S.-W., Su, Y., Kim, S., Cheng, H., Gur, O., Haney, R., Omenetto, F.G., Huang, Y., Rogers, J.A., 2013. Transient, biocompatible electronics and energy harvesters based on ZnO. Small 9 (20), 3398–3404.
Dakhlaoui, A., Jendoubi, M., Smiri, L.S., Kanaev, A., Jouini, N., 2009. Synthesis, characterization and optical properties of ZnO nanoparticles with controlled size and morphology. J. Cryst. Growth. 311 (16), 3989–3996.
Dinesha, M.L., Jayanna, H.S., Ashoka, S., Chandrappa, G.T., 2009. Temperature dependent electrical conductivity of Fe doped ZnO nanoparticles prepared by solution combustion method. J. Alloys Compd. 485, 538–541.
Dutta, R.K., Nenavathu, B.P., Gangishetty, M.K., Reddy, A.V., 2013. Antibacterial effect of chronic exposure of low concentration ZnO nanoparticles on *E. coli*. J. Environ. Sci. Health. Part A, Tox Hazard. Subst. Environ Eng. 48 (8), 871–878.
Elumalai, K., Velmurugan, S., Ravi, S., Kathiravan, V., Ashokkumar, S., 2015. Biofabrication of zinc oxide nanoparticles using leaf extract of curry leaf (*Murraya koenigii*) and its antimicrobial activities. Mater. Sci. Semicon. Proc. 34, 365–372.
Fazlzadeh, M., Rahmani, K., Zarei, A., Abdoallahzadeh, H., Nasiri, F., Khosravi, R., 2017. A novel green synthesis of zero valent iron nanoparticles (NZVI) using three plant extracts and their efficient application for removal of Cr (VI) from aqueous solutions. Adv. Powder Technol. 28 (1), 122–130.
Ficarra, R., Ficarra, P., Tommasini, S., Calabro, M., Ragusa, S., Barbera, R., Rapisarda, A., 1995. Leaf extracts of some Cordia species: analgesic and anti-inflammatory activities as well as their chromatographic analysis. Farmaco (Societa chimica italiana: 1989) 50 (4), 245–256.
Ghazanfar, S.A., 1994. Handbook of Arabian medicinal plants. CRC Press.
Kavyashree, D., Shilpa, C.J., Nagabhushana, H., Daruka Prasad, B., Sreelatha, G.L., Sharma, S.C., Ashoka, S., Anandakumari, R., Premkumar, H.B., 2015. ZnO Superstructures as an antifungal for effective control of malassezia furfur, dermatologically prevalent yeast: prepared by *Aloe Vera* assisted combustion method. ACS Sustain. Chem. Eng. 3 (6), 1066–1080.
Kirthi, A., Rahuman, A., Rajakumar, G., Marimuthu, S., Santhoshkumar, T., Jayaseelan, C., Velayutham, K., 2011. Acaricidal, pediculocidal and larvicidal activity of synthesized ZnO nanoparticles using wet chemical route against blood feeding parasites. Parasitol. Res. 109 (2), 461–472.
Kumari, R.M., Thapa, N., Gupta, N., Kumar, A., Nimesh, S., 2016. Antibacterial and photocatalytic degradation efficacy of silver nanoparticles biosynthesized using *Cordia dichotoma* leaf extract. Adv. Nat. Sci.: Nanosci. Nanotech. 7 (4), 045009.
Lakshmeesha, T.R., Sateesh, M.K., Prasad, B.D., Sharma, S.C., Kavyashree, D., Chandrasekhar, M., Nagabhushana, H., 2014. Reactivity of crystalline ZnO

superstructures against fungi and bacterial pathogens: synthesized using *Nerium oleander* leaf extract. Cryst. Growth Des. 14 (8), 4068–4079.
Lee, S.D., Nam, S.-H., Kim, M.-H., Boo, J.-H., 2012. Synthesis and photocatalytic property of ZnO nanoparticles prepared by spray-pyrolysis method. Phys. Procedia 32, 320–326.
Li, B., Wang, Y., 2009. Facile synthesis and enhanced photocatalytic performance of flower-like ZnO hierarchical microstructures. J. Phys. Chem. C. 114 (2), 890–896.
Li, M., Zhu, L., Lin, D., 2011. Toxicity of ZnO nanoparticles to *Escherichia coli*: mechanism and the influence of medium components. Environ. Sci. Technol. 45 (5), 1977–1983.
Matias, E.F.F., Alves, E.F., Do Nascimento Silva, M.K., De Alencar Carvalho, V.R., Coutinho, H.D.M., da Costa, J.G.M., 2015. The genus Cordia: botanists, ethno, chemical and pharmacological aspects. Rev. Bras. Farmaco. 25 (5), 542–552.
Nie, L., Gao, L., Feng, P., Zhang, J., Fu, X., Liu, Y., Yan, X., Wang, T., 2006. Three-dimensional functionalized tetrapod-like ZnO nanostructures for plasmid DNA delivery. Small 2 (5), 621–625.
Odoom-Wubah, T., Osei, W.B., Chen, X., Sun, D., Huang, J., Li, Q., 2016. Synthesis of ZnO micro-flowers assisted by a plant-mediated strategy. J. Chem. Technol Biotechnol. 91 (5), 1493–1504.
Pourmortazavi, S.M., Marashianpour, Z., Karimi, M.S., Mohammad-Zadeh, M., 2015. Electrochemical synthesis and characterization of zinc carbonate and zinc oxide nanoparticles. J. Mol. Struct. 1099, 232–238.
Qian, Y., Yao, J., Russel, M., Chen, K., Wang, X., 2015. Characterization of green synthesized nano-formulation (ZnO-A. vera) and their antibacterial activity against pathogens. Environ. Toxicol. Pharmacol. 39 (2), 736–746.
Qiu, Y., Chen, W., Yang, S., 2010. Facile hydrothermal preparation of hierarchically assembled, porous single-crystalline ZnO nanoplates and their application in dye-sensitized solar cells. J. Mater. Chem. 20 (5), 1001–1006.
Raghupathi, K.R., Koodali, R.T., Manna, A.C., 2011. Size-dependent bacterial growth inhibition and mechanism of antibacterial activity of zinc oxide nanoparticles. Langmuir 27 (7), 4020–4028.
Rajiv, P., Rajeshwari, S., Venckatesh, R., 2013. Bio-fabrication of zinc oxide nanoparticles using leaf extract of *Parthenium hysterophorus* L. and its size-dependent antifungal activity against plant fungal pathogens. Spectrochim. Acta A Mol. Biomol. Spectrosc. 112, 384–387.
Ramesh, M., Anbuvannan, M., Viruthagiri, G., 2015. Green synthesis of ZnO nanoparticles using *Solanum nigrum* leaf extract and their antibacterial activity. Spectrochim. Acta A Mol. Biomol. Spectrosc. 136 (Pt B), 864–870.
Raoufi, D., 2013. Synthesis and microstructural properties of ZnO nanoparticles prepared by precipitation method. Renew. Energy 50, 932–937.
Rasmussen, J.W., Martinez, E., Louka, P., Wingett, D.G., 2010. Zinc oxide nanoparticles for selective destruction of tumor cells and potential for drug delivery applications. Expert Opinion Drug Deliv. 7 (9), 1063–1077.
Sangeetha, G., Rajeshwari, S., Venckatesh, R., 2011. Green synthesis of zinc oxide nanoparticles by *Aloe barbadensis miller* leaf extract: Structure and optical properties. Mater. Res. Bull. 46 (12), 2560–2566.
Schmelzer, G.H., Gurib-Fakim, A., 2008. Medicinal Plants.
Senthilkumar, S., Sivakumar, T., 2014. Green tea (*Camellia sinensis*) mediated synthesis of zinc oxide (ZnO) nanoparticles and studies on their antimicrobial activities. Int. J. Pharm. Pharm. Sci. 6 (6), 461–465.
Sharma, D., Rajput, J., Kaith, B.S., Kaur, M., Sharma, S., 2010. Synthesis of ZnO nanoparticles and study of their antibacterial and antifungal properties. Thin Solid Films 519 (3), 1224–1229.
Sharma, R.K., Agarwal, M., Balani, K., 2016. Effect of ZnO morphology on affecting bactericidal property of ultra high molecular weight polyethylene biocomposite. Mater. Sci. Eng.: C 62, 843–851.
Sirelkhatim, A., Mahmud, S., Seeni, A., Kaus, N.H.M., Ann, L.C., Bakhori, S.K.M., Hasan, H., Mohamad, D., 2015. Review on zinc oxide nanoparticles: antibacterial activity and toxicity mechanism. Nano-Micro Lett. 7, 219–242.
Song, L., Zhang, S., Wu, X., Wei, Q., 2012. Controllable synthesis of hexagonal, bullet-like ZnO microstructures and nanorod arrays and their photocatalytic property. Ind. Eng. Chem. Res. 51, 4922–4926.
Suresh, D., Nethravathi, P.C., Udayabhanu, Rajanaika, H., Nagabhushana, H., Sharma, S.C., 2015a. Green synthesis of multifunctional zinc oxide (ZnO) nanoparticles using Cassia fistula plant extract and their photodegradative, antioxidant and antibacterial activities. Mater. Sci. Semicon. Proc. 31, 446–454.
Suresh, D., Shobharani, R.M., Nethravathi, P.C., Pavan Kumar, M.A., Nagabhushana, H., Sharma, S.C., 2015b. Artocarpus gomezianus aided green synthesis of ZnO nanoparticles: luminescence, photocatalytic and antioxidant properties. Spectrochim. Acta A Mol. Biomol. Spectrosc. 141, 128–134.
Talebian, N., Amininezhad, S.M., Doudi, M., 2013. Controllable synthesis of ZnO nanoparticles and their morphology-dependent antibacterial and optical properties. J. Photochem. Photobiol. B: Bio. 120, 66–73.
Tripathi, R.M., Bhadwal, A.S., Gupta, R.K., Singh, P., Shrivastav, A., Shrivastav, B.R., 2014. ZnO nanoflowers: novel biogenic synthesis and enhanced photocatalytic activity. J. Photochem. Photobiol. B: Bio. 141, 288–295.
Udayabhanu, Nagaraju, G., Nagabhushana, H., Basavaraj, R.B., Raghu, G.K., Suresh, D., Rajanaika, H., Sharma, S.C., 2016. Green, non chemical route for the synthesis of ZnO superstructures, evaluation of its applications towardsphotocatalysis, photoluminescence and bio-sensing. Cryst. Growth Des. 6 (12), 6828–6840.
Vafaee, M., Ghamsari, M.S., 2007. Preparation and characterization of ZnO nanoparticles by a novel sol–gel route. Mater. Lett. 61 (14–15), 3265–3268.
Vongsak, B., Sithisarn, P., Mangmool, S., Thongpraditchote, S., Wongkrajang, Y., Gritsanapan, W., 2013. Maximizing total phenolics, total flavonoids contents and antioxidant activity of Moringa oleifera leaf extract by the appropriate extraction method. Ind. Crops Prod. 44, 566–571.
Wang, L., Kang, Y., Liu, X., Zhang, S., Huang, W., Wang, S., 2012. ZnO nanorod gas sensor for ethanol detection. Sensors Actuators B: Chem. 162, 237–243.
Xiong, H.-M., 2013. ZnO nanoparticles applied to bioimaging and drug delivery. Adv. Mater. 25 (37), 5329–5335.
Yi, R., Zhang, N., Zhou, H., Shi, R., Qiu, G., Liu, X., 2008. Selective synthesis and characterization of flower-like ZnO microstructures via a facile hydrothermal route. Mater. Sci. Eng.: B 153 (1), 25–30.
Yuvakkumar, R., Suresh, J., Nathanael, A.J., Sundrarajan, M., Hong, S.I., 2014. Novel green synthetic strategy to prepare ZnO nanocrystals using rambutan (*Nephelium lappaceum* L.) peel extract and its antibacterial applications. Mater. Sci. Eng. C Mater. Biol. Appl. 41, 17–27.
Zhang, J., Wang, S., Wang, Y., Xu, M., Xia, H., Zhang, S., Huang, W., Guo, X., Wu, S., 2009. ZnO hollow spheres: preparation, characterization, and gas sensing properties. Sensors Actuators B: Chem. 139 (2), 411–417.
Zhang, L., Jiang, Y., Ding, Y., Povey, M., York, D., 2007. Investigation into the antibacterial behaviour of suspensions of ZnO nanoparticles (ZnO nanofluids). J. Nanoparticle Res. 9 (3), 479–489.
Zhao, X., Lou, F., Li, M., Lou, X., Li, Z., Zhou, J., 2014. Sol– gel-based hydrothermal method for the synthesis of 3D flower-like ZnO microstructures composed of nanosheets for photocatalytic applications. Ceram. Int. 40 (4), 5507–5514.
Zhou, J., Xu, N.S., Wang, Z.L., 2006. Dissolving behavior and stability of ZnO wires in biofluids: a study on biodegradability and biocompatibility of ZnO nanostructures. Adv. Mater. 18 (18), 2432–2435.